Title

A general framework for modeling subregional path effects

Authors
Buckreis, Tristan
Wang, Pengfei
Brandenberg, scott
et al.

Publication Date
2024-07-01

Peer reviewed

A GENERAL FRAMEWORK FOR MODELING SUBREGIONAL PATH EFFECTS

T.E. Buckreis[1], P. Wang[2], S.J. Brandenberg[3], & J.P. Stewart[3]

[1] Postdoctoral Scholar, University of California, Los Angeles, Los Angeles, CA, USA, tristanbuckreis@ucla.edu

[2] Assistant Professor, Old Dominion University, Norfolk, VA, USA

[3] Professor, University of California, Los Angeles, Los Angeles, CA, USA

Abstract: *Next Generation Attenuation (NGA) West2 ground motion models (GMMs) include regional path adjustments for broad jurisdictional regions, which necessarily averages spatially variable path effects within those regions. We extend that framework to account for systematic variations in attenuation within subregions defined in consideration of geologic differences. In recent years, cell-based methods which systematically account for spatial variations by summing the attenuation effects over a fine discretization of uniform-rectangular cells (e.g., Dawood and Rodriquez-Marek 2013; Kuehn et al. 2019) have been shown to be an effective alternative to regionalization and a step towards modelling non-ergodic path effects. The main drawbacks of these models, however, are their increased computational complexity, poorly informed coefficients for cells in which few paths travel, and unoptimized boundaries that may span across the limits of geologic domains. The framework presented here considers physio-geological differences to form subregional boundaries. Broad jurisdictional regions are divided into a number of subregions that are orders of magnitude greater in size than the uniform cells of cell-based methods, but smaller than regions corresponding to the NGA-West2 adjustments. Subregional boundaries are informed by geological differences and empirical observations to create domains with internally similar properties. The total attenuation effect for a given path that traverses multiple subregions is obtained by weighting the individual subregional effects by the proportion of the path length within each subregion. This approach has been successfully applied in California, where it was shown to achieve a reduction in bias and within-event and single-station variability relative to an NGA-West2 GMM for ground motions at large distance (R_{JB} > 100 km). The framework presented here can readily be adapted for other GMMs and regions.*

1. Introduction

Global ground motion models (GMMs) are developed from world-wide databases such that the scaling of ground motion predictor variables represents global averages. The principal drawback of global GMMs is that they have appreciable biases when applied to specific regions, which can partially be overcome by regionalizing certain model components. The Next Generation Attenuation (NGA) West2 GMMs include adjustments for broad jurisdictional regions, which necessarily averages spatially variable effects within those regions. These models reduce bias, however within-region biases are still present. An interesting question for ground motion analysts is what degree of regionalization is justified by data trends and regional properties.

In this paper, we provide an overview of different approaches to model path effects, in which we present a general framework for modeling subregional path effects. At a high-level, a subregional approach attempts to model variable path effects across some domain as a continuum by accounting for systematic effects. The method by which individual subregions are defined is an integral part of the overall framework. Therefore, we discuss different types of information that can be used to develop subregional boundaries (i.e., subregionalization). For each type of information, we provide examples to illustrate how the information can be used.

2. Overview of Different Approaches to Model Path Effects

Path models (F_P) can be expressed in the following general form:

$$F_P(\boldsymbol{M}, R) = c_1(\boldsymbol{M})\ln(R) + c_2 R \quad (1)$$

where the first and second terms represent the geometric spreading and anelastic attenuation, respectively; R is a distance parameter (e.g., closest distance, R_{rup}, or Joyner-Boore distance, R_{JB}); $c_1(\boldsymbol{M})$ represents the magnitude-dependent geometric spreading coefficients; and c_2 represents the anelastic attenuation coefficient. Coefficients $c_1(\boldsymbol{M})$ and c_2 may be considered fixed (global) coefficients. In this section we provide an overview of three popular approaches to modeling path effects: (1) regional or local, (2) cell-specific, and (3) subregional methods.

2.1. Regional

Regional or local anelastic path models are commonly developed for regions where there is ample ground motion data to quantify regional-deviations from the global coefficients, and can be generically expressed as:

$$F_P(\boldsymbol{M}, R, region) = c_1(\boldsymbol{M})\ln(R) + (c_2 + \Delta c_2)R \quad (2)$$

where Δc_2 represents the region-specific anelastic attenuation adjustment conditioned on $region$. In the context of these models, a region represents a broad scale (e.g., Japan, Italy, California). This modeling approach has been sucessfully implemented in the NGA-West2 GMMs (e.g., Abrahamson et al. 2014; Boore et al. 2014; Campbell and Bozorgnia 2014; Chiou and Youngs 2014), and on smaller-local scales for areas with densly sampled data (e.g., in the San Francisco Bay Area by Erdem et al. 2019). The advantages of these models are their computational simplicity, ability to capture region-specific path effects, and ease of interpretation (i.e., path effects can be attributed to regional properties). However, systematic path effects that may vary across the region are averaged together into a single Δc_2 value, meaning that within-region predictions may be biased for individual paths, but as a whole are unbiased.

2.2. Cell-Specific

Dawood and Rodriquez-Marek (2013) originally proposed the cell-specific approach, in which a study domain is discretized into non-overlapping cells, to systematically account for path-dependent effects within the domain. The generic cell-specific path model formulation can be expressed as:

$$F_P(\boldsymbol{M}, \overrightarrow{\Delta R}) = c_1(\boldsymbol{M})\ln(R) + \sum_{i}^{N_c} \Delta c_{2,i}\, \Delta R_i \quad (3)$$

in which N_c is the number of cells; $\Delta c_{2,i}$ is the anelastic attenuation coefficient for cell i; ΔR_i is the path length within the ith cell; and $\overrightarrow{\Delta R}$ is an array of all ΔR_i ($\sum_i^{N_c} \Delta R_i = R$). Accordingly, the contribution of F_P in the GMM is unique for any given path.

This approach requires a large number of earthquakes recorded by a dense array of strong motion stations to be able to constrain the cell-specific anelastic attenuation coefficients. Kuehn et al. (2019) succsessfully applied this method in California using 30 x 30 km cells, as illustrated in Figure 1(b). The advantage of this approach is that it separates systematic path effects from event and site effects in areas having densly sampled data, as evident by the blue (slower-than-average attenuation) and red (faster-than-average attenuation) shading compared to the state-wide average (white) as derived via a regional approach (Figure 1a). Challenges associated with the application of this approach are data limitations that cause cell-specific coefficients to be poorly constrained, and a substantial increase in the complexity of ground motion calculations due to the large number of cells that need to be considered. Moreover, the gridded cell boundaries are not optimized to capture the limits of geologic domains, which may lead to the mixing of variable path effects within a single cell, and are not easily interpretable (i.e., why do certain cells possess faster-than-average attenuation, while others exhibit slower-than-average?).

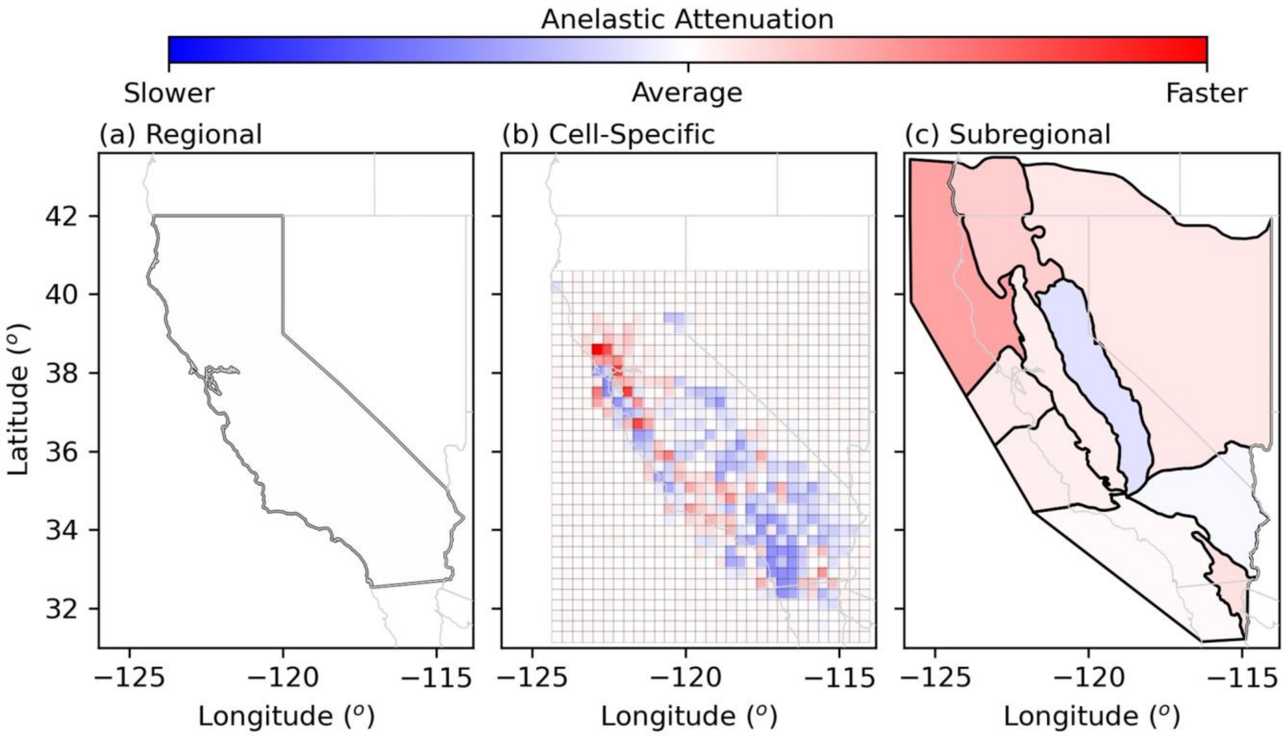

Figure 1. Comparing (a) regional (e.g., Boore et al. 2014), (b) cell-specific (Kuehn et al. 2019), and (c) subregional (Buckreis et al. 2023) approaches to modelling anelastic path effects. Shading corresponds to zones of slower-than-average (blue) and faster-than-average (red) anelastic attenuation.

2.3. Subregional

The subregional method proposed by Buckreis et al. (2023) is conceptually similar to the cell-specific method, however draws on subregionalization representative of crustal and path-related features instead of uniform cells. A generic subregional path model can be expressed as:

$$F_P(\boldsymbol{M}, R, \overrightarrow{W_r}) = c_1(\boldsymbol{M})\ln(R) + (c_2 + \Delta c_2^*)R \tag{4}$$

where

$$\Delta c_2^* = \sum_r^{N_R} \Delta c_{2,r}\, W_r \tag{5}$$

in which N_R is the number of subregions; $\Delta c_{2,r}$ is the anelastic attenuation adjustment for subregion r; W_r is the proportion of the path within subregion r ($W_r = \Delta R_r / R$); and $\overrightarrow{W_r}$ is an array of all W_r ($\sum_r^{N_R} W_r = 1.0$). Alternatively, a subregional path model can be expressed as:

$$F_P(\boldsymbol{M}, \overrightarrow{\Delta R}) = c_1(\boldsymbol{M})\ln(R) + \sum_r^{N_R}(c_2 + \Delta c_{2,r})\,\Delta R_r \tag{6}$$

Subregionalization is discussed in detail in the following section, however the objective is to identify areas which exhibit similar path-effects on which the path model can be conditioned. The advantage of this approach is that individual elements (i.e., subregions or cells) are representative of similar characteristics, and are not arbitrarily defined. Furthermore, subregions can be irregular and vary in size meaning that areas with densely sampled data can be finely discretised, whereas areas with sparsely sampled data can be coarse, resulting in well constrained estimates across the entire study domain.

This approach has been successfully applied in California using 10 broad subregions by Buckreis et al. (2023). Figure 1(c) compares the relative rates of subregional attenuation to the regional and cell-based results for California. The subregions used in Buckreis et al. (2023) are orders of magnitude greater in size than the cells used by Kuehn et al. (2019), however similar trends are observed (e.g., slower-than average attenuation in the eastern portions of the state and higher-than average attenuation along the northern-coastal areas). The results presented by Buckreis et al. (2023) suggest that further refinement of the subregionalization in certain areas of the state (e.g., southern California) may be needed.

3. Subregionalization

A major aspect of the subregional approach is the way in which model developers subdivide the domain into distinct subregions. In general, subregions should characterize an area which exhibits compatible crustal attenuation, and is rooted by physical properties. In this section we present different types of information that may be considered when discretizing a domain into subregions. These considerations include broad-physiographic provinces, detailed models of crustal properties (e.g., rock-quality factor), and geologic information as well as empirical observations through event-specific residual and spatial analyses. It is important to note that these types of information are intended to aid in discretizing a study domain into distinct subregions, and are not necessarily the only types of information that can be considered.

3.1. Physiographic Provinces

Physiographic provinces are defined as regions having particular geomorphic features (e.g., topography, geologic structure, and processes of landforms) that differ significantly from that of adjacent regions. This type of information is convenient for subregionalization, because it can provide initial starting blocks that are derived from physical attributes that may or may not relate to path effects. For example, California can be divided into 13 separate provinces which distinguish hilly-areas collocated with relatively straight portions of the San Andreas plate boundary, major inland mountainous areas, and major basin structures – shown in Figure 2. On their own, these provinces do not provide insight into systematic path effects within a region. However, when combined with other types of information, such as that described subsequently, they can be used to define subregional boundaries.

3.2. Q_S Models

Rock-quality factor (Q_S) describes anelastic attenuation in which $1/Q_S$ is the fractional loss of energy per cycle, and may relate to lithology, deformation, fluid, and thermal effects. Low Q_S is associated with faster rates of attenuation (i.e., paths traversing through more fractured or fluid materials), while high Q_S is associated with slower rates of attenuation (i.e., paths traversing through more-competent materials). Three-dimensional Q_S models are developed for many regions, including California, and can be used to infer spatial trends of anelastic attenuation. Such models are depth-dependent, as illustrated in Figure 2 for California, which presents the variation of Q_S across the state at different depth horizons proposed by Eberhart-Phillips (2016). Overlain on the Q_S maps depicted in Figure 2 are outlines of the 13 physiographic provinces discussed in the previous section.

The maps shown in Figure 2 can be used to identify areas which possess low, intermediate, and high levels of Q_S to inform subregionalization. These results can be interpreted on their own, or to check the significance of physiographic province boundaries. For example, the Sierra Nevada province exhibits higher-than-average Q_S (suggestive of slower attenuation) at depths less than 20 km, which is the depth range where most earthquake waves will travel as they propagate to any given site in this tectonic regime. This observation suggests that the Sierra Nevada province may be an appropriate subregion within the context of path modelling. On the other hand, the Coastal Range is shown to have variable levels of Q_S, with areas of low Q_S being concentrated in the northern portions of the province and intermediate levels towards the south. These observations suggest that the Coastal Range province should be further divided to accurately capture the within-province path effects. While this discussion focused on the combined insights of physiographic provinces and Q_S maps, it is equally valid to consider Q_S maps on their own.

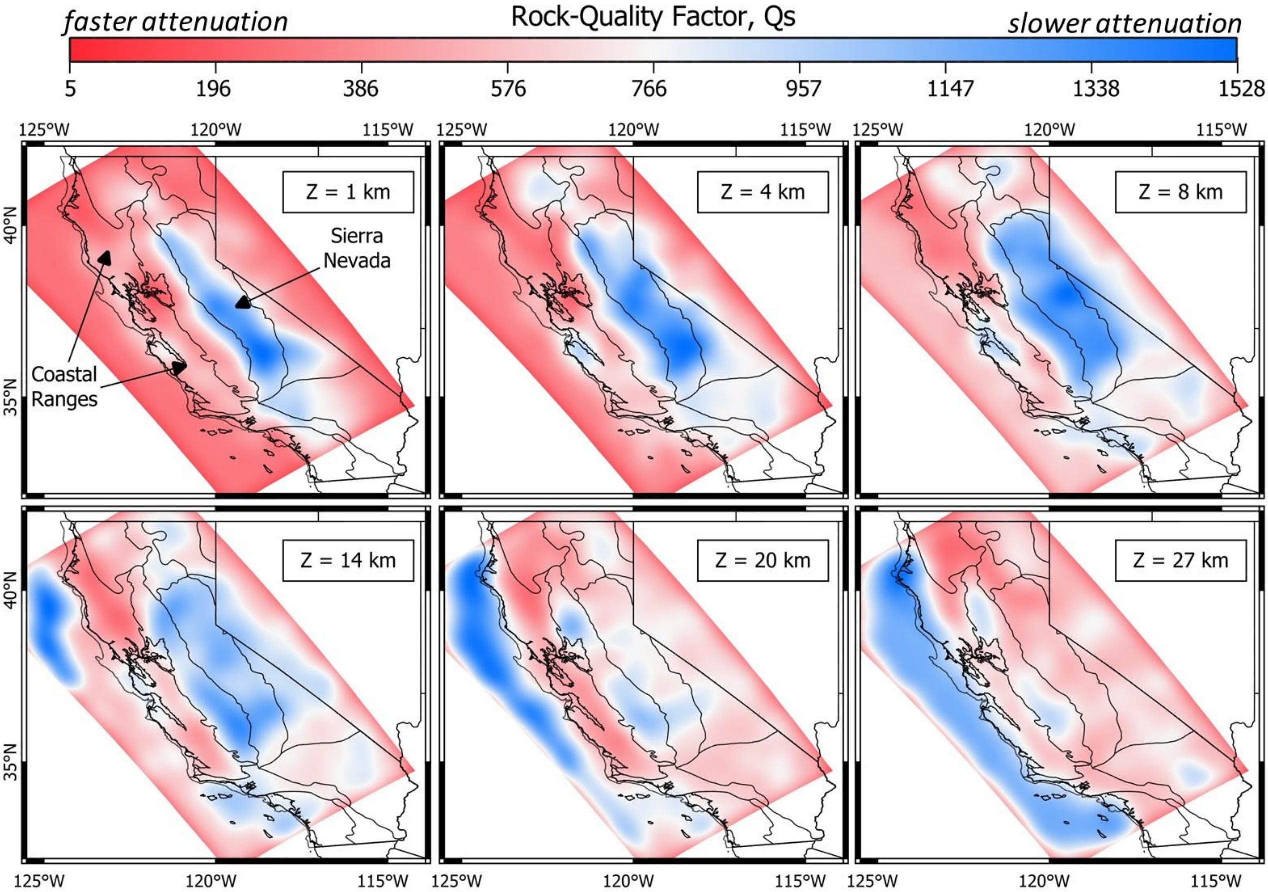

Figure 2. Maps of rock-quality factor (Q_S) from Eberhart-Phillips (2016) at different depth horizons. Low Q_S (red shading) correspond to regions interpreted to have higher rates of attenuation, and high Q_S (blue shading) correspond to regions interpreted to have lower rates of attenuation. Solid-black lines represent outlines of physiographic provinces.

3.3. Geology

Geologic considerations represent a broad field of information which can be used to inform subregionalization, however in this subsection we focus only on two aspects: (1) lithology and (2) structural geology. We begin first with lithology, which is concerned with the physical and chemical properties of rocks and soils. Materials of similar composition can be expected to possess similar anelastic properties. While this is not always the case, there is some evidence to show that there usually is some correlation. For example, the Sierra Nevada province shown in Figure 2 corresponds to the Sierra Nevada batholith, which we previously stated as having relatively high Q_S values (suggestive of slower attenuation). While this is true across the region as a whole, closer inspection of Figure 2 reveals a slightly decreasing gradient in Q_S values from the south to the north within the province. This can somewhat be explained by lithology, because the rocks in the south are younger than those in the north (i.e., more competent and intact materials, which relate to higher Q_S, are expected in the south) (Bateman 1992). Therefore, the geologic composition of crustal materials can be used to help inform subregional boundaries.

Whereas lithology is useful for identifying the spatial extents of individual subregions, structural geology can be used to pinpoint exact boundaries between neighboring subregions. Faults represent a facture between two blocks of rocks, and therefore provide clear discontinuities. To illustrate the potential utility of major faults as subregional boundaries, we consider the cell-based $\Delta c_{2,i}$ values proposed by Kuehn et al. (2019) because this model provides relatively fine discretization across the state and can be easily compared to locations of known faults. Figure 3 presents maps of $\Delta c_{2,i}$ for PSA at 1.0 sec and peak ground velocity (PGV) along with the locations of known major faults in California. For both intensity measures, there is a general trend of slower attenuation (blue shading) on the Pacific plate immediately to the southwest of the San Andreas Fault (SAF), and faster attenuation (red shading) immediately to the northeast on the North American plate. These trends become less consistent as the distance increases from the fault, suggesting that the SAF may serve as an appropriate subregional boundary. Comparable trends are also observed at smaller-scales near other major faults (e.g., Hayward and Calaveras Faults in northern California).

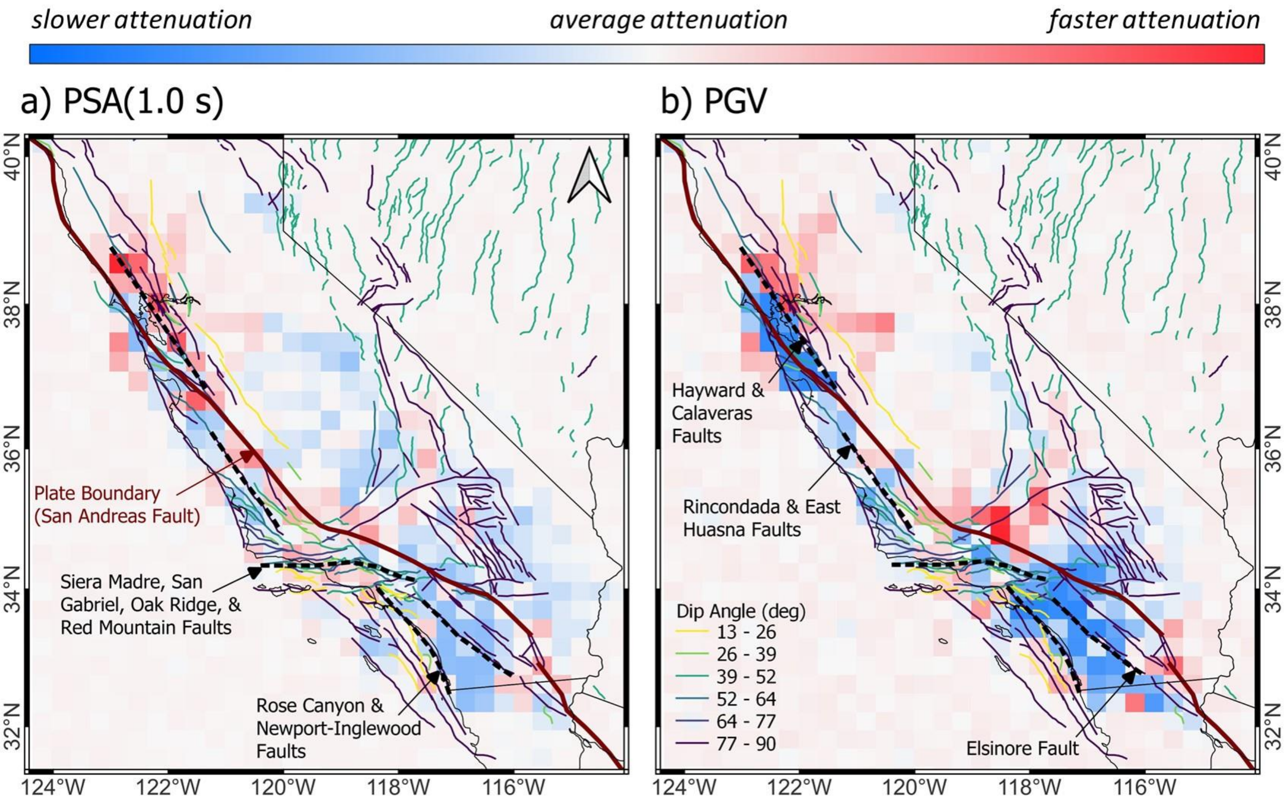

Figure 3. Maps of California structural features (major faults) with trends of (a) PSA(1.0 sec) and (b) PGV relative anelastic attenuation ($\Delta c_{2,i}$) from Kuehn et al. (2019).

It is important to indicate that the inferences made from Figure 3 represent a combination of geologic properties (i.e., locations of faults) and empirical models (e.g., relative rates of anelastic attenuation from a published study). These inferences serve to provide evidence that major structural features may be good options for subregional interfaces, however this is not always the case. For example, the Elsinore fault in southern California does not appear to serve as a clear boundary between strongly different relative rates of attenuation. This does not necessarily mean that the Elsinore fault cannot serve as a dividing boundary, however the neighboring subregions can likely be characterized as having similar $\Delta c_{2,r}$, and therefore may benefit by being merged. These types of decisions are left up to model developers.

3.4. Empirical Observations

Whereas the previous considerations can be examined for any study area (provided the necessary information is available), this sub-section focus on empirical observations and can therefore only be examined in areas with sufficient recorded earthquake ground motion data.

Residuals and Event-Specific Attenuation

Total residuals (R_{ij}) represent the difference between data and the median prediction of a GMM,

$$R_{ij} = \ln\left(Y_{ij}\right) - \mu_{ij}(\boldsymbol{M_i}, R_{JB,ij}, V_{S30,j}, \ldots) \quad (7)$$

where $\ln\left(Y_{ij}\right)$ is the natural logarithm of the observed intensity measure at site j from event i; and μ_{ij} is the natrual log median prediction from a GMM conditioned on the indicated parameters. Total residual R_{ij} can be partitioned using mixed-effects analyses (Abrahamson and Youngs 1992):

$$R_{ij} = c_k + \eta_{E,i} + \delta W_{ij} \quad (8)$$

where k is an index for the GMM; $\eta_{E,i}$ is the event term which quantifies bias attribued to source effects; and δW_{ij} represents the within-event residual.

When path models are biased, trends in residuals (both R_{ij} and δW_{ij}) with respect to distance are observed, which contaminate $\eta_{E,i}$ in the sense that these event terms do not solely reflect source attributes (Baltay et al. 2020). For example, residual observations of PSA at 1.0 sec from the February 6, 2023 **M**7.8 Pazarcik, Türkiye earthquake show a relatively horizontal trend to distances of up to approximately 200 km, beyond which the path model of the selected GMM (Boore et al. 2014) under-predicts attenuation (Figure 4a). In order to obtain accruate estimates for $\eta_{E,i}$, we only consider observations up to a limiting distance within which the trend of residuals with distance are relatively flat (e.g., R < 200 km) whenever path-biases are observed.

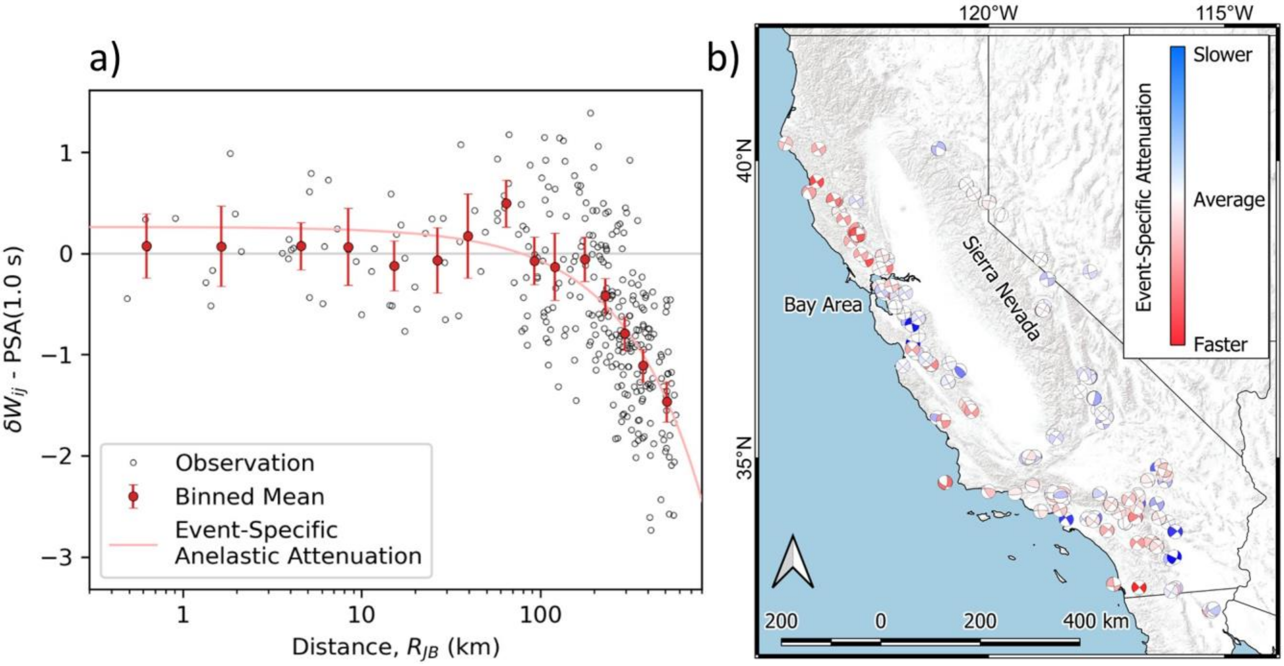

*Figure 4. (a) Plot of within-event residuals (PSA at 1.0 sec) versus distance for the February 6, 2023 **M**7.8 Pazarcik, Türkiye earthquake with event-specific anelastic attenuation (Eqn. 9); (b) spatial variation of event-specific attenuation in California for PGA [adapted from Buckreis et al. 2023].*

As a means to quantify and visualize differences in attenuation trends spatially, we perform event-specific regressions as follows:

$$\delta W_{ij} = \Delta c_2^i \,(R - R_{ref}) + \Delta c_0^i \qquad (9)$$

where Δc_2^i is an adjustment to c_2 for event i; Δc_0^i represents a constant term which allows the function to shift vertically to fit the data; and R_{ref} = 1 km. An example fit is provided in Figure 4(a) for δW_{ij} for PSA at 1.0 sec from the **M**7.8 Pazarcik, Türkiye earthquake. Results for well-recorded events (i.e., sufficient number of recordings over a wide distance-range) in California from Buckreis et al. (2023) are plotted in Figure 4(b). From these results, we observe that the majority of the events north of the Bay Area exhibit negative Δc_2^i values, suggestive of the region possessing faster-than-average attenuation. Conversely, many of the events to the east of the Sierra Nevada mountain range possess positive Δc_2^i values, suggestive of the region possessing slower-than-average attenuation. These observations provide evidence of systematic path effects manifesting over relatively large subregions.

Spatial Analysis of Well-Recorded Events

It is important to note that event-specific attenuation is representative of all paths that radiate from the earthquake, and does not discriminate based on any particular subregion. That being said, attenuation trends inferred from the type of analysis discussed above may be controlled by properties of several neighboring subregions. One can partially overcome this limitation by binning the data by azimuth, which results in the regressed anelastic coefficients becoming event-and-azimuth dependent. However, an even better approach may be to rigorously examine the spatial trends of δW_{ij}. It stands that the added complexity of spatial analyses only provides additional benefits when there is substantial data to confidently assess trends over a relatively large area, and is not feasible for all earthquakes.

Correlation models can be developed for δW_{ij} that consider between-station closeness in Euclidean distance and azimuthal distance (relative to the earthquake epicenter) (e.g., Bodenmann et al. 2023). Applying these models with ordinary Kriging can produce maps that describe the spatial variation of δW_{ij}. This type of analysis has been implemented for the **M**7.8 Pazarcik, Türkiye earthquake, which is known to have significant path effects (Figure 4a) (Buckreis et al. 202x). Figure 5 presents the derived mean δW_{ij} map for PSA at 1.0 sec, which illustrates that weaker-than-average observations (blue) tend to be to the north-west of the rupture, while stronger-than-average observations (red) tend to be to the south-east. Although δW_{ij} contain a combination of site-specific and path biases, one can postulate that broad spatial trends in δW_{ij} are characteristic of path bias. For the present example, this is supported by the fact that the trends shown in Figure 5 align with the trend seen in Figure 4(a) since the majority of the distant observations (R > 200 km) are to the northwest of the rupture.

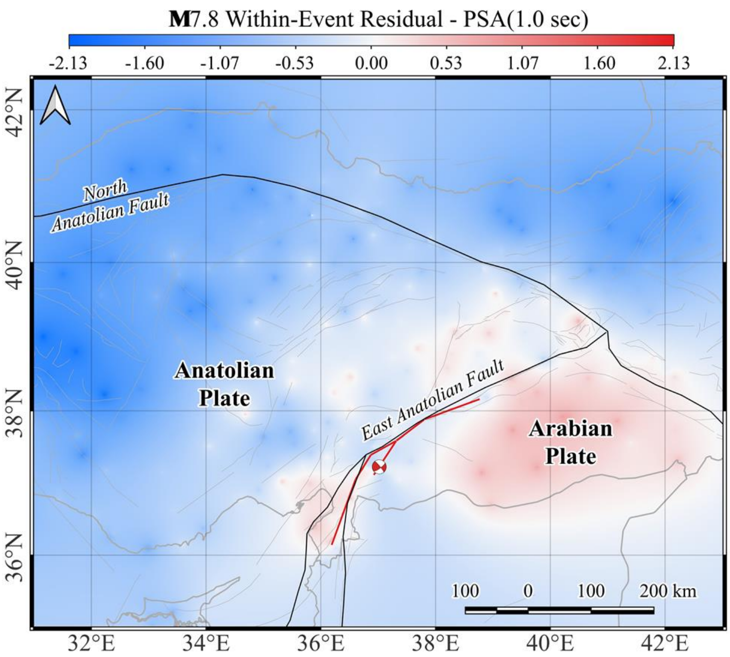

*Figure 5. Spatial variation of the mean within-event residual (PSA at 1.0 sec) for February 6, 2023 **M**7.8 Pazarcik, Türkiye earthquake in Figure 4(a); blue and red shading indicated areas of weaker- and stronger-than-average ground motions, respectively [adapted from Buckreis et al. 202x].*

Although spatial analyses of well recorded events are not intended to be used to define subregions, it stands that their results may be used to support subregionalization in some instances. In the case of the February 2023 Türkiye earthquake sequence, similar results as shown in Figure 5 are observed across multiple events and intensity measures (Buckreis et al. 202x). When these observations are combined with physical attributes of the region (e.g., tectonic plate interfaces), there is strong evidence of tectonic block-dependent anelastic attenuation in the region (i.e., faster attenuation on the Anatolian plate and slower attenuation on the Arabian plate). It stands that future path models for Türkiye should consider these as distinct subregions, which may be further subdivided if needed. However, similar analyses should be performed after updating the path models to assess whether or not the trends persist or go away. If the trends are observed after updating the path model, it could be that they were incorrectly attributed to anelastic effects. Therefore, caution should be exercised when using these types of analyses to inform subregionalization.

4. Summary and Conclusions

We present a framework to model subregional anelastic path effects which considers geologic differences across a region. Mathematically, a subregional model in application is identical to a cell-based one, however the individual elements (subregions or cells) have underlying physical bases. Subregionalization, which is the method by which a region is subdivided, should take into consideration multiple types of information (e.g., geomorphology, geology, and empirical observations) whenever possible. This framework has been demonstrated to be effective at capturing spatially variable path effects across California, and can be applied in other regions. Subregional path models represent a refinement to ergodic, region-specific path models, and are expected to be useful for regional hazard analyses and non-ergodic site response applications

5. References

Abrahamson N.A., Silva W.J., Kamai R. (2014). Summary of the ASK14 ground motion relation for active crustal regions, *Earthquake Spectra*, 30(3): 1025-1055.

Abrahamson N.A., Youngs R.R. (1992). A stable algorithm for regression analyses using the random effects model, *Bulletin of the Seismological Society of* America, 82: 505–510.

Baltay A.S., Abrahams L.S., Hanks T.C. (2020). When source and path components trade-off in ground-motion prediction equations, *Seismological Research Letters*, 91(4): 2259-2267.

Bateman P.C. (1992). Plutonism in the central part of the Sierra Nevada Batholith, California, *U.S. Government Printing Office*, Issue 1483.

Bodenmann L., Baker J.W., Stojadinovic B. (2023). Accounting for path and site effects in spatial ground-motion correlation models using Bayesian inference, *Natural Hazards and Earth System Sciences* 23: 2387–2402.

Boore D.M., Stewart J.P, Seyhan E., Atkinson G.M. (2014). NGA-West2 equations for predicting PGA, PGV, and 5%-Damped PSA for Shallow Crustal Earthquakes, *Earthquake Spectra*, 30: 1057-1085.

Bozorgnia Y., Abrahamson N.A., Al Atik L., Ancheta T.D., Atkinson G.M., Baker J.W., Baltay A., Boore D.M., Campbell K.W., Chiou B.S.-J., Darragh R. (2014). NGA-West2 research project, *Earthquake Spectra* 30: 973-987.

Buckreis T.E., Pretell R., Sandikkaya M.A., Kale Ö., Askan A., Brandenberg S.J., Stewart J.P. (202x). Engineering attributes of ground motions from February 2023 Türkiye earthquake sequence, *Earthquake Spectra*, (submitted).

Buckreis T.E., Stewart J.P., Brandenberg S.J., Wang P. (2023). Subregional anelastic attenuation model for California, *Bulletin of the Seismological Society of America*, DOI: 10.1785/0120220173.

Campbell K.W., Bozorgnia Y. (2014). NGA-West2 ground motion model for the average horizontal components of PGA, and 5% damped linear acceleration response spectra, *Earthquake Spectra*, 30(3): 1087-1115.

Chiou B., Youngs R., Abrahamson N., Addo K. (2010). Ground motion attenuation model for small-to-moderate Shallow Crustal Earthquakes in California and its implications on regionalization of ground-motion prediction models, *Earthquake Spectra*, 26: 907-926.

Chiou B.-S.J., Youngs R.R. (2014). Update of the Chiou and Youngs NGA model for the average horizontal component of peak ground motion and response spectra, *Earthquake Spectra*, 30(3): 1117-1153.

Dawood H.M., Rodriguez - Marek A. (2013). A method for including path effects in ground - motion prediction equations: An example using the Mw 9.0 Tohoku Earthquake aftershocks, *Bulletin of the Seismological Society of America*, 103(2B): 1360–1372.

Eberhart-Phillips D. (2016). Northern California seismic attenuation: 3D QP and QS models, *Bulletin of the Seismological Society of America*, 106(6): 2558-2573.

Erdem J.E., Boatwright J., Fltecher J.B. (2019). Ground-motion attenuation in the Sacramento-San Joaquin Delta, California, from 14 Bay Area earthquakes, including the 2014 M 6.0 South Napa earthquake, *Bulletin of the Seismological Society of America*, 109(3): 1025-1033.

Kuehn N.M., Abrahamson N.A., Walling M.A. (2019). Incorporating nonergodic path effects into the NGA-West2 ground-motion prediction equations, *Bulletin of the Seismological Society of America*, 109(2): 575-585.